

Current Performance and Future Practices in FPSO Hull Condition Assessments

Mark Tammer⁽¹⁾, *Mirosław Lech Kaminski*⁽²⁾, *Myriam Koopmans*⁽²⁾, *JianJung Tang*⁽²⁾

(1) Institute for Engineering & Design, Faculty of Natural Sciences and Technology, HU University of Applied Sciences Utrecht, The Netherlands.

(2) Ship Hydromechanics and Structures, Maritime and Transport Technology, Faculty of Mechanical, Maritime and Materials Engineering, Delft University of Technology (TU-Delft), The Netherlands.

ABSTRACT

The aim of this paper is to show the benefits of enhancing classic Risk Based Inspection (without fatigue monitoring data) with an Advisory Hull Monitoring System (AHMS) to monitor and justify lifetime consumption to provide more thorough grounds for operational, inspection, repair and maintenance decisions whilst demonstrating regulatory compliance.

KEY WORDS: FPSO Inspection; Advisory Hull Monitoring System (AHMS), Non-Destructive Testing (NDT); Risk Based Inspection (RBI); Structural Health Monitoring (SHM); Condition Based Maintenance (CBM).

INTRODUCTION

Floating Production Storage and Offloading units (FPSOs) are being recognized as one of the most economical systems to exploit marginal and (ultra) deep-water area's (Paik and Tayamballi, 2007). With the increasing of the size, complexity and economic interests of these units, emphasis lies on the optimization of design, construction and operation in order to achieve high levels of functional integrity in terms of Safety, Health and Environmental (SHE) factors, and life-cycle capital (CAPEX) and operational (OPEX) expenditures.

FPSO structures pose some difficulties in contrast to traditional fixed offshore structures and trading tankers, as the units have a very large displacement volume and are continuously operated under (benign) site-specific environmental conditions, endure high levels of loading and offloading cycles, are equipped with mooring systems and can experience dynamic impacts from sloshing, green water, wave slamming and shuttle tanker collision and generally lack the ability to dry-dock. In order to safeguard structural integrity and fatigue lifetime consumption, calculations are required to detect and predict structural deterioration before a possibly catastrophic, polluting and/or expensive failure can result (Tammer and Kaminski, 2013).

Current FPSO design, construction and maintenance practices rely on traditional structural inspection methods as a primary instrument to identify and mitigate system anomalies and unanticipated defects. Logically, during the service life of a unit a small Probability of Failure is inevitable due to the complexity of the design, construction and operational characteristics, as well as from the economic principle of reasonableness. This Probability of Failure is usually managed

through periodical inspections of specific details and is combined with the Consequence of Failure to provide a risk profile and inspection scheme to prevent incidents and maintain a specific safety level. Conversely, unnecessary, disruptive and costly inspection and maintenance could lead to high costs, downtime, subsequent damage and inherent Safety, Health and Environmental issues and should be prevented as much as possible. Hence, an optimum exists, which should be approximated as well as possible.

Risk Based Inspection (RBI) can be depicted as an emerging methodology, playing an inevitable role in determining this optimum with respect to fatigue degradation of FPSO hulls. The methodology focuses on more directed inspection effort to the most critical risk profiles through a generalisation principle. This further strengthens the case for correct inspection results, as these form one of the constitutes for the (future) integrity management and inspection plans. However, inspection (activities) intrinsically include fundamental limitations. In general, inspection performance relies on the available resources, skills, methods and inspection frequency, which pose challenges. It is argued that the use of Structural Health Monitoring can provide for a damage detection- and characterization strategy to overcome (most of) these issues.

Risk Based Inspection

In order to operationalize residual fatigue life-calculations and performance- and compliance based inspection regimes, the quantification and qualification of risks and the affiliated thresholds is essential. Traditionally, design data, historical records, input from 'comparable' assets, expert judgment, Non-Destructive Evaluation/Testing (NDE/NDT), (limited) probabilistic modelling and industry and legal standards are used to determine (initial) regimes. After gaining experience from the initial and subsequent inspections, degradation patterns for probabilistic models can be constructed. These models are able to produce estimations and predictions about asset degradation and structural integrity at a specific time in the future. By linking this understanding of degradation propagation with the classification of the inherent risks of this process and the consequences of failure, a more specific assessment and risk ranking can be made as an alternative for standard (prescribed) practices - which could be unsuitable for a specific asset design and/or operational context (over- or under stringent). Hence, the practice which is referred to as Risk Based Inspection (Tammer and Kaminski, 2013).

Although RBI for FPSOs is noticeably adopted by all major stakeholders and refined tools for determining Residual Fatigue Life on hull structures with fatigue as a primary degradation mechanism exist, publications on the detailed procedural combination and application are still very limited. Therefore this work describes a detailed demonstrator case study and can be seen as a successor of the paper 'Fatigue Oriented Risk Based Inspections of FPSOs' by Tammer and Kaminski (2013).

RBI Fatigue Assessment

Naturally and as stated, other damage mechanisms besides fatigue contribute, or may even dominate and dictate the inspection frequency. However, this differs per specific asset and situation. For example, newly-build or specifically enhanced structures may not encounter corrosion issues. Therefore, please note that in this specific demonstrator case the scope is limited to fatigue damage.

The scope in terms of these structural details is made specific in close collaboration with the Maritime Research Institute Netherlands (MARIN) to provide a comparable case for (1) the application of RBI without monitoring data (classic RBI) and (2) with Monitas input (which will be referred to as 'enhanced RBI'). The background of the Monitas system is described by Kaminski (2007) and the Monitas methodology and -application are discussed in more detail by Aalberts, Van der Cammen and Kaminski (2010), L'Hostis, Van der Cammen, Hageman and Aalberts (2013) and Van der Meulen and Hageman (2013).

The next step consist of a comparison between both cases and the deployed tools to explicitly show the benefits of applying RBI in combination with an Advisory Hull Monitoring System (in this paper the Monitas system). In concreto: The reduction of uncertainty and hence the Probability of Failure and elongation or shortening of the inspection interval. Ergo, validate the assumption that using Monitas data for RBI reduces the methodological uncertainty to provide better predictive values. Besides the differences in classic and enhanced RBI, the case is also focused on the differences in parameter selection and tuning process. Summarized, this paper elucidates upon the total procedure, outcomes and distinctions/differences of RBI step 3 as outlined by Tammer and Kaminski (2013) in detail.

Crack Growth Assessment

For the crack growth assessment the Fracture Mechanics approach is applied with the Paris-Erdogan (1963) crack growth model:

$$\frac{da}{dn} = C(\Delta K)^m \quad [1]$$

using the following notations:

- a - depicts the crack length
- n - the number of stress cycles
- K - the stress intensity factor range
- C - the crack growth intercept parameter
- m - the crack growth slope parameter

The left hand side represents the crack length increment in one stress cycle with the stress intensity factor range at the crack tip K . The stress intensity factor range is defined as the difference between the maximum and the minimum stress intensity factor during a load cycle, which is a measure of the magnitude of the stress near the crack tip.

K is expressed as:

$$\Delta K = \Delta\sigma \cdot Y\{a\} \cdot \sqrt{\pi a} \quad [2]$$

where $Y\{a\}$ is the geometry function depending on the crack length and the overall geometry of the joint, including the presence of the weld. With equation 2, equation 1 can be rewritten as:

$$\frac{da}{(Y\{a\}\sqrt{\pi a})^m} = C(\Delta\sigma)^m dn \quad [3]$$

Subsequently, a 2-parameter Weibull distribution approach can be used to determine the loading. The Weibull cumulative distribution function of the stress range $\Delta\sigma$ is denoted as:

$$F(\Delta\sigma) = 1 - \exp\left(-\left(\frac{\Delta\sigma}{A}\right)^B\right) \quad [4]$$

where:

- A - depicts the scale parameter and
- B - the shape parameter.

The number of stress cycles is determined by:

$$n = v_0 \cdot T \cdot F(\Delta\sigma) = v_0 \cdot T \left(1 - \exp\left(-\left(\frac{\Delta\sigma}{A}\right)^B\right)\right) \quad [5]$$

where v_0 denotes the number of stress cycles over time $T = T_{\text{end}} - T_{\text{beg}}$. Substituting equation 5 into equation 3 and integrating both sides results in:

$$\int_{a_{\text{beg}}}^{a_{\text{end}}} \frac{da}{(Y\{a\}\sqrt{\pi a})^m} = \int_0^\infty v_0 \cdot T \cdot C(\Delta\sigma)^m \frac{B}{A} \left(\frac{\Delta\sigma}{A}\right)^{B-1} \exp\left(-\left(\frac{\Delta\sigma}{A}\right)^B\right) d(\Delta\sigma) \quad [6]$$

where a_{beg} - denotes the crack length at the crack growth initiation at the time T_{beg} and a_{end} the crack length at the time T_{end} .

Now, equation 6 can be evaluated by application of the following integral result:

$$\int_0^\infty x^a \exp(-x^b) dx = \frac{1}{b} \Gamma\left(\frac{a+1}{b}\right) \quad [7]$$

and the right hand of equation 6 can be written as:

$$\begin{aligned} \int_0^\infty v_0 \cdot T \cdot C(\Delta\sigma)^m \frac{B}{A} \left(\frac{\Delta\sigma}{A}\right)^{B-1} \exp\left(-\left(\frac{\Delta\sigma}{A}\right)^B\right) d(\Delta\sigma) \\ = \int_0^\infty v_0 \cdot T \cdot C \cdot a_m \\ \cdot B \left(\frac{\sigma}{A}\right)^{m+B-1} \exp\left(-\left(\frac{\Delta\sigma}{A}\right)^B\right) d\left(\frac{\Delta\sigma}{A}\right) \\ = v_0 \cdot T \cdot C \cdot a_m \cdot \Gamma\left(1 + \frac{m}{B}\right) \end{aligned} \quad [8]$$

Combining equation 6, 7 and 8 provides us with:

$$\int_{a_{beg}}^{a_{end}} \frac{da}{(Y\{a\}\sqrt{\pi a})^m} = v_0 \cdot C \cdot a_m \cdot \Gamma\left(1 + \frac{m}{B}\right) (T_{end} - T_{beg}) \quad [9]$$

The left hand sides of equation 3 and 8 represents the resistance, which is also referred to as damage and the right hand sides the loading, which is also known as the damaging effect. Now, the reliability state function can be defined as:

$$M(a_{beg}, a_{end}, T_{beg}, T_{end}) = \int_{a_{beg}}^{a_{end}} \frac{da}{(Y\{a\}\sqrt{\pi a})^m} - v_0 \cdot C \cdot a_m \cdot \Gamma\left(1 + \frac{m}{B}\right) (T_{end} - T_{beg}) \quad [10]$$

Qualitative Effects of Inspections

The arbitrary data presented in table 1 is used in order to demonstrate the qualitative effects of inspections on the reliability of a single component. The calculations are performed with the DNV Sesam Probability software package and the results are displayed in figure 1:

Variable	Name	Distribution	Mean	SD	unit
a_0	Initial crack length	Exponential	1	1	mm
a_m	Measured crack length	Normal	4	1	mm
a_d	Detectable crack length	Exponential	2	2	mm
a_c	Critical crack length	Normal	50	1	mm
T_1	Time of first Inspection	Fixed	10	-	year
T_2	Time of second Inspection	Fixed	20	-	year
v_0	Average stress range annual frequency	Fixed	1.E+06	-	1/year
$\ln(C)^*$	Material crack growth rate offset constant	Normal	-29.75	0.5	***
m^*	Material crack growth rate slope constant	Normal	3	0.3	-
$\ln(A)^{**}$	Weibull stress range scale parameter	Normal	2.94	0.14 7	***
$1/B^{**}$	Weibull stress range slope parameter	Normal	0.877	0.04 4	-
$Y(a)$	Geometrical function	Fixed	1	-	-

Table 1 - Stochastic model

*Correlation Values -0.9, **Correlation Values -0.79, *** stress in MPa, crack length in mm, SD – standard deviation

Figure 1 shows variations of the annual safety index of a structural component over the time interval of 30 years. It was assumed that the target reliability equals 2. This requires a first inspection at the 10th year. A ‘no crack detection’-inspection scenario results in an acceptable safety level until the 20th year. When the second inspection at this year detects a crack of 4mm, the safety threshold is already unacceptable after 2 years (at year 22). Hence, this implies maximum Time To Repair of 2 years.

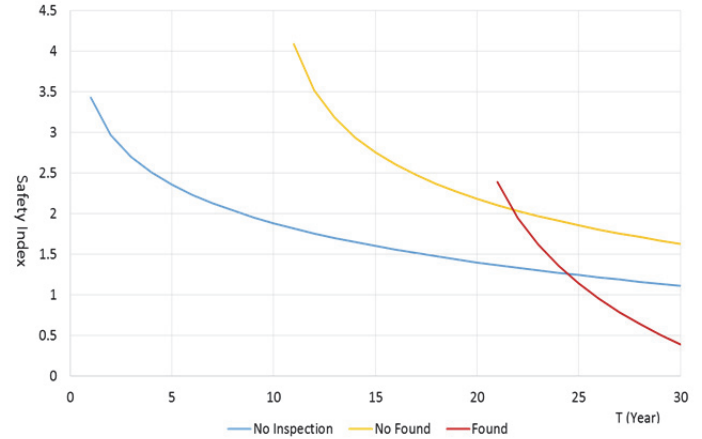


Figure 1 – Effect of inspection on component safety

Sensitivity Study

The safety level depends on the mean and the standard deviation values of variables influencing the fatigue failure. Figure 2 and 3 show the variation of the safety index during the lifetime without inspection when the c.o.v. (coefficient of variance = standard deviation/mean) of $\ln(A)$ changes from 5% to 50% and from 1% to 10% respectively. The safety index shows a high sensitivity to this c. o. v. It is expected that the Monitas system will reduce the c. o. v. of $\ln(A)$ and therefore will increase the safety level, even if the mean $\ln(A)$ would remain the same.

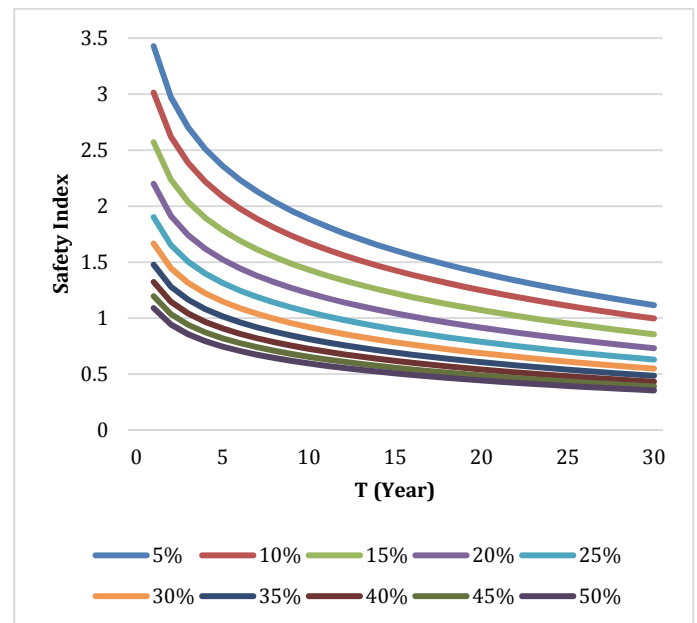


Figure 2 – Effect of c. o. v. of $\ln(A)$ on the safety index level

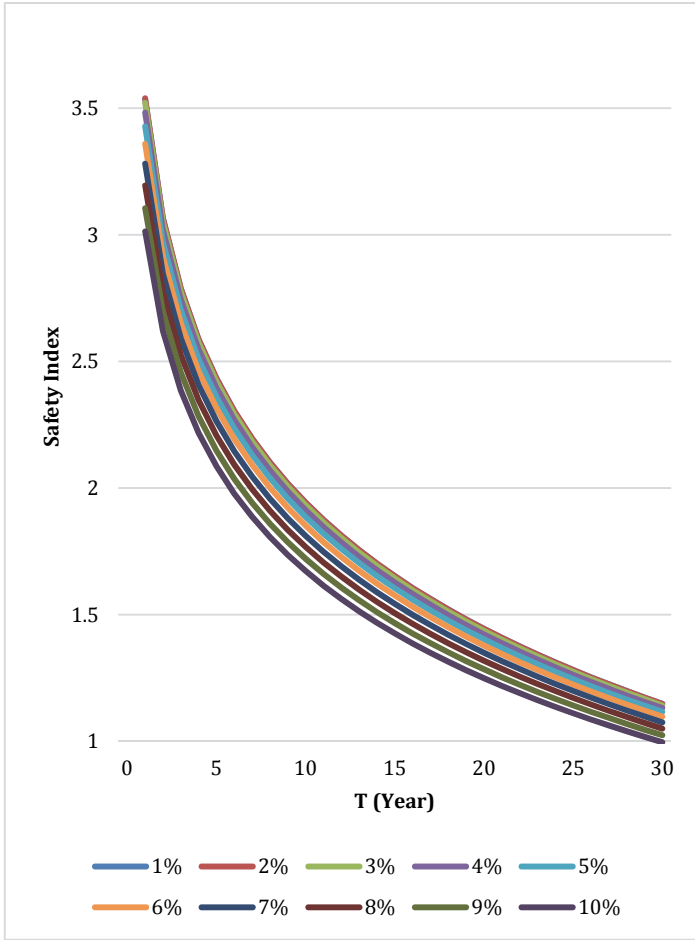


Figure 3 – Effect of c. o. v. of $\ln(A)$ on the safety index level

Calibration

Before the inspection planning can be optimised using the reliability analysis, the stochastic model of the Fracture Mechanics (FM) has to be calibrated in such a way that the safety levels calculated using both approaches (SN-approach used in the design and FM-approach used in RBI) are the same at a given time, e.g. at the design lifetime (or over the whole lifetime as proposed by Straub, 2004).

The limit function for the S-N approach is:

$$M(t) = \eta - \frac{v_0 t}{K} a_m \cdot \Gamma\left(1 + \frac{m}{B}\right) \quad [11]$$

and the limit function for the FM approach is:

$$M(a_{beg}, a_{end}, T_{beg}, T_{end}) = \int_{a_{beg}}^{a_{end}} \frac{da}{(X \cdot Y\{a\} \sqrt{\pi a})^m} - v_0 \cdot C \cdot a_m \cdot \Gamma\left(1 + \frac{m}{B}\right) (T_{end} - T_{beg}) \quad [12]$$

Thereafter, three calibration parameters and several combinations are applied:

- The geometrical function parameter X
- The Initial crack length a_0 and
- The material crack growth rate offset constant $\ln(A)$

The arbitrary data presented in subjoined table 2 are applied in order to demonstrate the calibration process:

Variable	Unit	Distribution	Mean	Dispersion
SN-approach – resistance part				
$\log(K)$	Stress in MPa	Normal	12.6	SD = 0.2
m^{SN}	-	Fixed	3.0	-
η	-	Log-normal	1.60	SD = 0.3
FM-approach – resistance part				
a_0	mm	Exponential	0.11	SD = 0.1
a_c	mm	Fixed	20.0	-
X	-	Log-normal	1.00	SD = 0.1
Y	-	Fixed	1	-
$\ln(C)$	Stress in MPa Crack in mm	Normal	-31.0	SD = 0.77
m^{FM}	-	Fixed	3.0	-
Common loading part				
$\ln(A)$	Stress in MPa	Normal	2.9	c.o.v. = 5%
B	-	Fixed	0.95	-
v_0	Hz	Fixed	0.13	-
T	s	Fixed	20 years	-

Table 2 - Stochastic model for FM calibration

To limit computational time, 4 safety indexes are calculated instead of the whole lifetime, since the result shows adequate accuracy. Thus, safety indexes are calculated for the 1st, 7th, 13th and 19th year. Equation 13 shows the calibration function. The goal is to find a value of the calibration parameter, which minimizes the value of S .

$$S = (\beta_{SN}^1 - \beta_{FM}^1)^2 + (\beta_{SN}^7 - \beta_{FM}^7)^2 + (\beta_{SN}^{13} - \beta_{FM}^{13})^2 + (\beta_{SN}^{19} - \beta_{FM}^{19})^2 \quad [13]$$

The results of calibration are showed in subjoined figures. Firstly, figure 4 shows the effect of varying the mean of parameter X of the geometrical function between 0.5 and 1.2. The minimal value of S is 1.353 for $X = 0.57$:

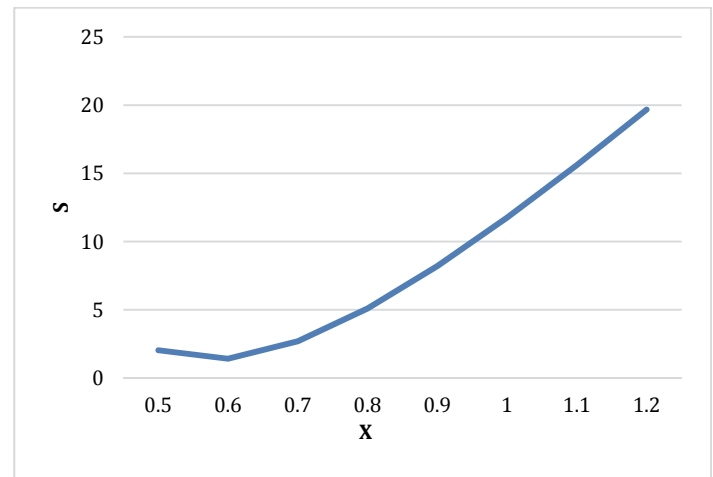


Figure 4 – Calibration applying the mean of parameter X of the geometrical function

Subjoined figure 5 shows the effect of varying the mean of initial crack length a_0 between 0.1 and 0.3. The value S is decreasing gradually, which indicates that a larger initial crack size provides a better calibration fit. The minimal value of S is 2.75 for the initial crack length of 0.3. Subsequent calculations need to be carried out in order to find the minimal value of S . In this case, it is expected that the initial crack length of 0.4 would result in the minimal value of S equal to 2.0.

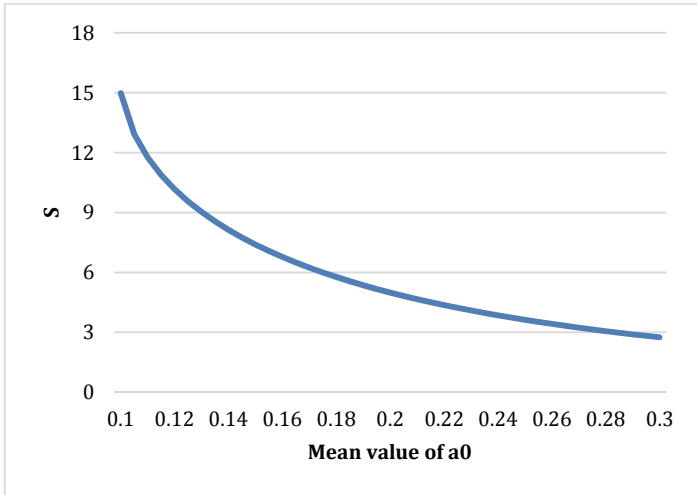


Figure 5 – Calibration using the mean of initial crack length

Figure 6 shows the effect of varying the multiplier of material crack growth rate offset constant $\ln(C)$ between 0.982 and 1.054. S is reaching its lowest point (1.351) at the multiplier equal to 1.053.

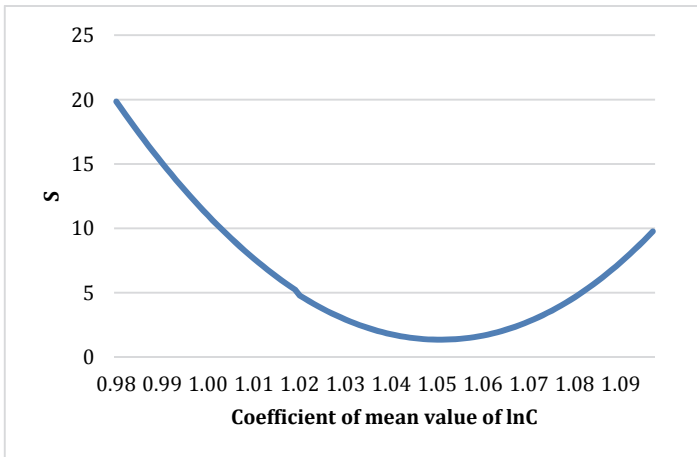


Figure 6 – Calibration using the multiplier of material crack growth rate offset constant

From the three considered cases, the calibration using parameter X of the geometrical function gives the best result (i.e. the minimal value of S). Then the optimal solution for $X = 0.57$ is presented in figure 7.

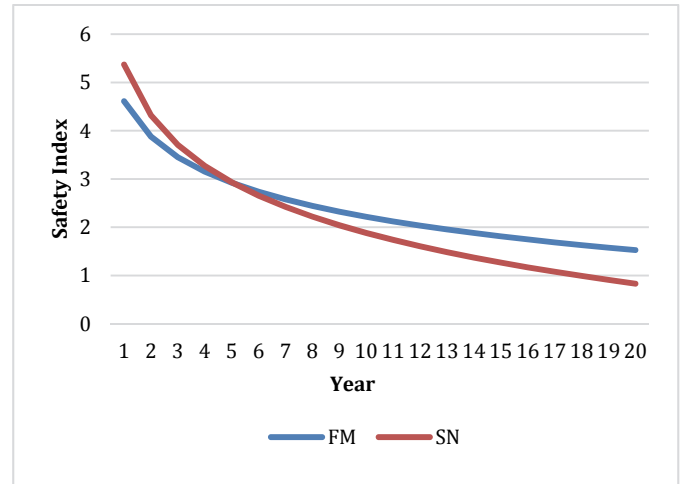


Figure 7 – Result of FM calibration

Hence, the calibration results can be improved by using two variables instead of a single variable. Figure 8 shows the effect of varying the mean of initial crack length a_0 between 0.1 and 0.2 for $X = 0.57$. Now, the optimal solution $S = 1.29$ is obtained for a_0 equal to 0.115, which is shown in figure 9.

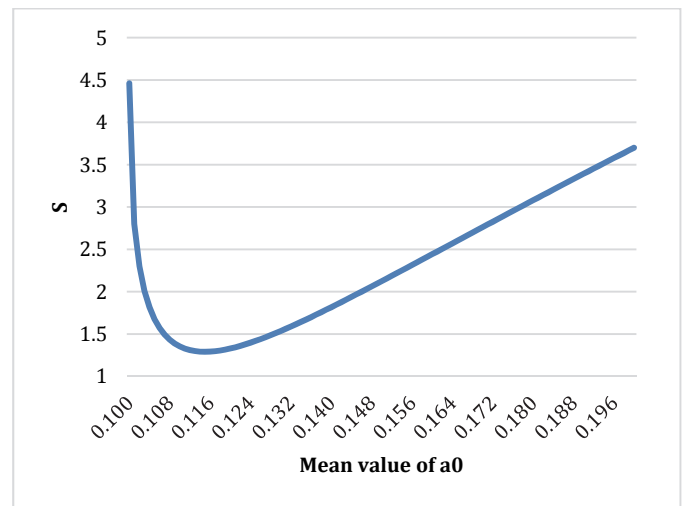


Figure 8 – Optimal X calibration using the mean of the initial crack length

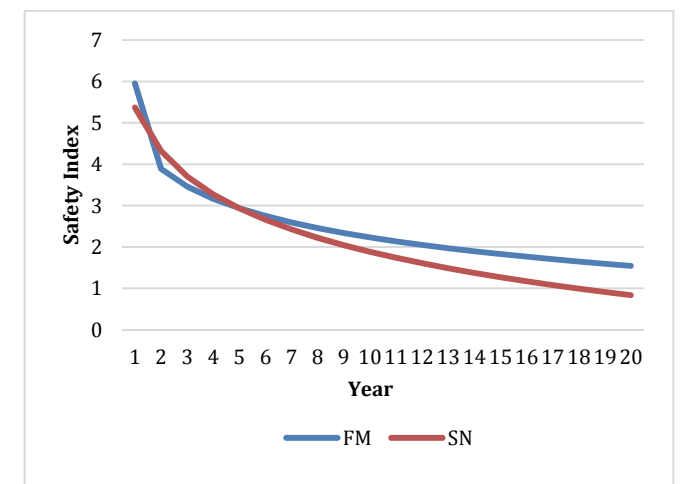


Figure 9 – Result of the calibration with two variables

Now, it can be concluded that the parameter X of the geometrical function and the initial crack length are very efficient calibration parameters, which can be considered as the primary and the secondary calibration parameter.

Effect of Monitas data on RBI results

The Monitas system estimates the Weibull distribution parameters of the long-term stress ranges based on measurements. This distribution is described by the parameters A and B , as given in equation 4. In order to demonstrate the effect of Monitas data on the RBI results different data sets of A and B are considered:

- Arbitrary data given in table 1 (in order to compare trends);
- Reconstructed design data (based on known fatigue damage using equation 14);
- Design data known (using full hydro-structural calculations);
- As-measured by Monitas;
- As-forecasted by Monitas using the measured and the design data.

Firstly, it has been assumed that c.o.v.'s are constant and equal to 0.05. These data sets are summarized in the table 3 and the results shown in figure 10. Where O (Original) represents the used arbitrary design data, DFD the Design only FDF and M the measured data.

Case A	mean	\ln mean	c.o.v.	SD
A - Arbitrary data	18.91	2.940	0.05	0.147
R - Reconstructed design data	6.658	1.895	0.05	0.095
D - Design data	9.120	2.210	0.05	0.111
M - Measured data	7.402	2.001	0.05	0.100
F - Forecast data	8.890	2.184	0.05	0.109
Case B	mean	\ln mean	c.o.v.	SD
A - Arbitrary data	1.140	0.877	0.05	0.0440
R - Reconstructed design data	0.937	1.068	0.05	0.0536
D - Design data	1.172	0.853	0.05	0.0428
M - Measured data	1.128	0.887	0.05	0.0445
F - Forecast data	1.168	0.856	0.05	0.0430

Table 3 - Weibull parameters of the long-term stress range distribution for different data sets (constant c.o.v.)

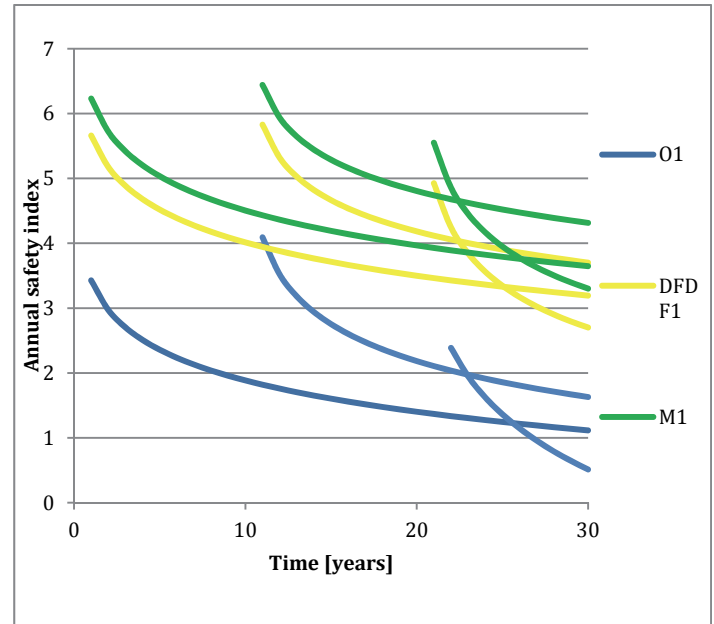


Figure 10 – General effects of Monitas data on RBI (constant c.o.v.)

Now, an equal trend of all reliability curves is noticed, indicating that the scale parameter of the Weibull distribution ($\ln A$) shifts the curves up or down depending on its values. It is obvious that, when measured stress ranges are lower (represented by lower $\ln A$) the safety improves by representation of higher annual safety index values. It is observed that a short monitoring period (in the present case 2 years) hardly affects the design reliability curves.

However, this comparison is incomplete, as it is reasonable to assume that the uncertainty of the calculations is a factor 2 in comparison to the measurement uncertainty. Therefore, subsequently it has been assumed that the design data have a double c.o.v. (e.g. 0.1). Naturally, the choice of a factor 2 is arbitrary and additional research is a necessity to provide better estimations. The data sets are summarized in table 4. Peruse that the mean values of the reconstructed data slightly differ in table 3 and 4. The results are shown in figure 11 - note that only 'no-inspection' lines are plotted.

Case A	mean	\ln mean	c.o.v.	SD
A - Arbitrary data	6.580	1.884	0.100	0.188
R - Reconstructed design data	9.120	2.210	0.100	0.221
D - Design data	7.402	2.001	0.050	0.100
M - Measured data	8.890	2.184	0.075	0.164
F - Forecast data	6.580	1.884	0.100	0.188
Case B	mean	\ln mean	c.o.v.	SD
A - Arbitrary data	0.850	1.176	0.100	0.1176
R - Reconstructed design data	1.172	0.853	0.100	0.0853
D - Design data	1.128	0.887	0.050	0.0444
M - Measured data	1.168	0.856	0.075	0.0642
F - Forecast data	0.850	1.176	0.100	0.1176

Table 4 - Weibull parameters of the long-term stress range distribution for different data sets (varying c.o.v.)

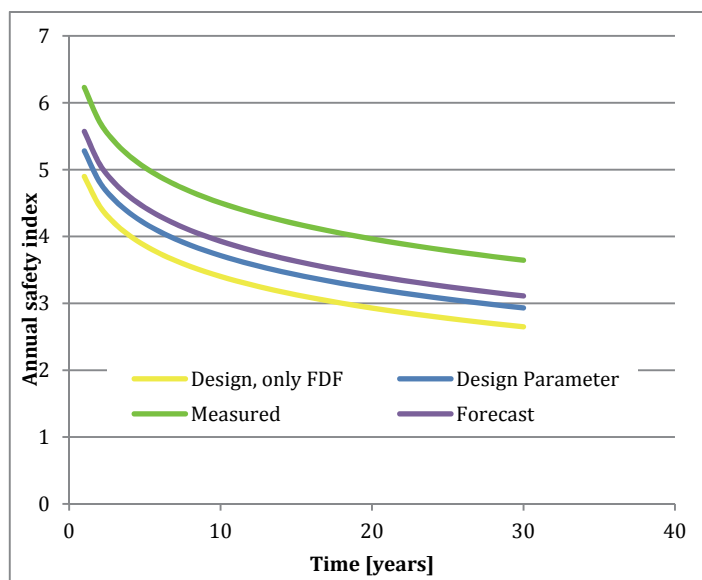


Figure 11 – General effects of Monitas data on RBI (varying c.o.v.)

It can be now seen that the Monitas data improves the safety by reducing the uncertainty of long term stress range distribution - i.e. reduction of c.o.v. of $\ln(A)$. This is equally important as the proper estimation of stress range values. Hence, estimation of the $\ln(A)$ mean value.

CONCLUSION

The goal of this research was to explore how the Risk Based Inspection methodology can benefit from an AHM-system. The field of investigation has been restricted to fatigue failure of a single structural welded detail. In order to reach this goal, a reliability-model has been built based on the Fracture Mechanics approach, which allows for several successive inspections.

First, without considering the Monitas AHMS-data it has been demonstrated that the model can be deployed to optimize the inspection schedule in such a way that the annual reliability index of a structural detail will not drop below its allowable threshold value. In order to keep the reliability model consistent with the conventional design method based on the SN-approach, a calibration process has been introduced. This process modifies 2 Fracture Mechanics parameters (primarily the geometrical fraction, and secondarily the initial crack size) in such a way that the differences between the obtained reliability from both approaches are minimized. This process can be seen as a quality check, assuring that a relatively sensitive reliability model is not (mis)used in obtaining results.

As stated, conventional Risk Based Inspection applies design and desk data. Therefore, its uncertainty is relatively high. The use of monitoring data should reduce this uncertainty and improve the

credibility of RBI-predictions by linking the long-term stress range distribution - which is successively aggregated by the Monitas system and a prerequisite in the reliability model for calculating. Ergo, for maintaining the annual safety levels. This link has been explored in this document through cases and data sets including design-, monitoring- and forecast data.

Finally, it is concluded that this link improves the credibility of the advice provided by RBI due to the lower uncertainty (standard deviation, c.q. coefficient of variation) of the parameters describing the long-term stress range distribution. To this moment, most research efforts have been focused on the accurate estimation parameters' mean values. Therefore, it is recommended to direct subsequent research efforts in the estimation of the standard deviations of these parameters to further enhance the methodology.

REFERENCES

- Aalberts, P.J., Cammen, Van der, J. and Kaminski, M.L. (2010). The Monitas System for the Glas Dour FPSO. In: OTC 20873 - Proceedings of the Offshore Technology Conference. 3-6 May 2010. Houston, Texas: USA.
- Kaminski, M.L. (2007). Sensing and understanding Fatigue Lifetime of New and Converted FPSOs. In: OTC18913 - Proceedings of the 2007 Offshore Technology Conference. 30 April - 3 May 2007. Houston, Texas: USA.
- L'Hostis, D., Kaminski, M.L., Aalberts, P.J. (2010). Overview of the Monitas JIP. In: OTC 20872 - Proceedings of the Offshore Technology Conference. 3-6 May 2010. Houston, Texas: USA.
- L'Hostis, D., Cammen, Van der, J., Hageman, R.B. and Aalberts, P.J. (2013). Overview of the Monitas II Project. Proceedings of the 23rd International Offshore and Polar Engineering Conference (ISOPE). 1 - 5 July. Anchorage: Alaska.
- Meulen, Van der, F.H. and Hageman, R.B. (2013). Fatigue Predictions using Statistical Inference within the Monitas II JIP. Proceedings of the 23rd International Offshore and Polar Engineering Conference. 1 - 5 July. Anchorage: Alaska.
- Paik, J.K. and Thayamballi, A.K. (2007). Ship-shaped Offshore Installations - Design, Building and Operation. Cambridge University Press. Cambridge: United Kingdom. ISBN: 978-0-521-18788-6.
- Paris, P. C., & Erdogan, F. (1963). A Critical Analysis of crack Propagation Laws. Journal of Basic Engineering 85(4) pp. 528-533.
- Straub, D. (2004). Generic Approaches to Risk Based Inspection Planning for Steel Structures [online PhD dissertation]. Institute of Structural Engineering, Swiss Federal Institute of Technology, ETH Zürich. Available from: <http://e-collection.library.ethz.ch/eserv/eth:1550/eth-1550-01.pdf>
- Tammer, M.D., and Kaminski, M. L. (2013). Fatigue Oriented Risk Based Inspection and Structural Health Monitoring of FPSOs. Proceedings of the 23rd International Offshore and Polar Engineering Conference (ISOPE) pp. 438-449. June 30-July 5, 2013. Anchorage, Alaska: USA.